

KATANA — a charge-sensitive trigger/veto array for the S π RIT TPC

P. LASKO^{(1)(2)(*)}, J. BRZYCHCZYK⁽²⁾, P. HIRNYK, J. ŁUKASIK⁽¹⁾, P. PAWŁOWSKI⁽¹⁾,
K. PELCZAR⁽²⁾, A. SNOCH⁽³⁾, A. SOCHOCKA⁽²⁾ and Z. SOSIN^{(2)†}

⁽¹⁾ *IFJ PAN - Kraków, Poland*

⁽²⁾ *Institute of Physics, Jagiellonian University - Kraków, Poland*

⁽³⁾ *University of Wrocław - Wrocław, Poland*

received 10 January 2017

Summary. — KATANA — the Kraków Array for Triggering with Amplitude discrimination, has been built and used as a trigger and veto detector for the S π RIT TPC at RIKEN. Its construction allows operating in magnetic field, providing fast response for ionizing particles and giving the approximate multiplicity and charge information on forward emitted reaction products. Depending on this information, trigger and veto signals are generated. Multi-Pixel Photon Counters were used as light sensors for plastic scintillators. Custom designed front-end and peripheral electronics will be presented as well.

1. – Introduction

The symmetry term in the Nuclear Equation of State (NEoS) is being recently intensively investigated [1, 2]. The experimental efforts are focused on constraining the stiffness of the symmetry energy, especially in the range of higher densities [3]. One of the proposed methods consists in getting the information on momentum distribution of charged pions and isotopically-resolved light charged particles, $Z \leq 3$, emitted in the central heavy-ion collisions [4-6]. Realization of this kind of measurements inspired the construction of the Time Projection Chamber (TPC) called S π RIT (the SAMURAI Pion-Reconstruction and Ion-Tracker) [7, 8].

To obtain sufficiently large gas amplification for pions and light charged particles, a high electric field is required inside the chamber. This brings a danger of damage when a heavier fragment passes through the chamber: charge produced by gas ionization can

(*) E-mail: pawel.lasko@ifj.edu.pl

† Deceased.

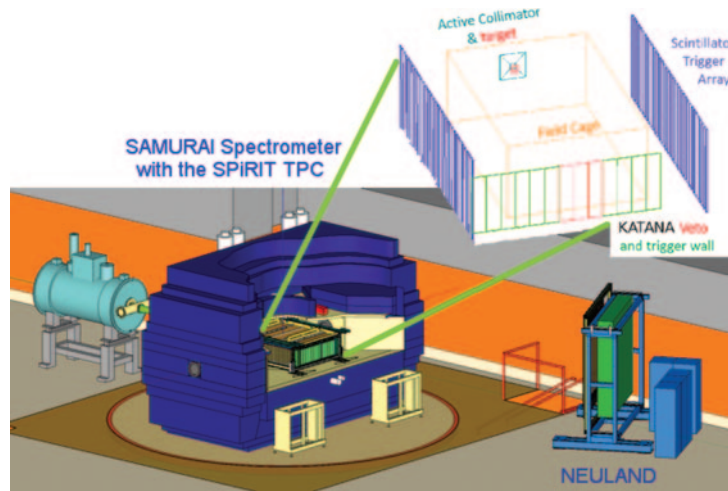


Fig. 1. – $S\pi$ RIT experimental setup.

exceed safe limit for the pad planes of the TPC. For this reason, a gating grid wire plane was mounted in front of the pad plane [7]. The grid is normally closed, but may be quickly opened (in ~ 200 ns) when an interesting collision occurs.

The KATANA array has been designed to play a double role: to produce a minimum bias or a given multiplicity trigger and to provide a veto signal whenever a beam particle or a fragment heavier than $Z \simeq 20$ has passed through the chamber. To fulfill the requirements, the wall has been constructed of two parts, a Veto and Trigger arrays. The KATANA-Veto part consisting of 3 thin (1 mm thick) plastic-scintillator paddles with the middle one centered on the beam, has been designed to produce a veto signal for heavy fragments. The KATANA-Trigger array, consisting of 12 thicker (10 mm thick) paddles, arranged on both sides of the beam, has been designed to produce a trigger.

This paper will shortly describe details of the KATANA wall construction and of the accompanying electronics. More details on the performance of the detector will be presented in [9, 10].

2. – Experimental setup

The experimental setup [11] is depicted in fig. 1 with the $S\pi$ RIT TPC as the main detection device. The TPC was placed inside the SAMURAI super-conducting spectrometer [12] at Rare Isotope Beam Facility (RIBF) of RIKEN [13].

The target was located about 3 mm upstream of the field cage within the $S\pi$ RIT enclosure. The KATANA detector was located downstream of the exit TPC window. In this configuration HI beam first hits the target, than fragments pass through the chamber and finally reach KATANA paddles. An additional active collimator detector was applied upstream of the target to reduce the rate of the out-of-target events. On both sides of the TPC additional triggering KYOTO arrays were installed to provide a central-event trigger. Neutrons were detected with the NeuLand [14] detector.

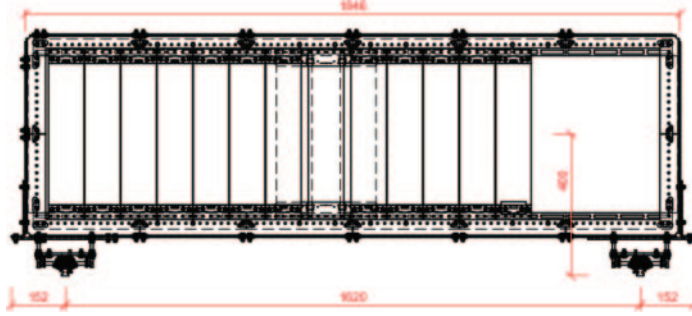


Fig. 2. – KATANA detector: a technical drawing with external dimensions (in mm).

3. – KATANA detector — overall description

The design of KATANA detector is schematically presented in fig. 2. Three veto plastic bars, marked with dashed lines, (size $400 \times 100 \times 1 \text{ mm}^3$, made of BC404) are placed in about the middle of the frame. Twelve trigger plastics ($400 \times 100 \times 10 \text{ mm}^3$, made of BC408) are placed unevenly on both sides of the beam (7 on the left and 5 on the right side) to account for bending of the charged particles in the magnetic field.

The scintillators are fixed to the frame by two handles. For the thick paddles the light is collected by two light sensors, each located in the middle of the top and bottom side of the plastic. The light is read out directly, without any light-guides. The handles for the thin veto paddles have more complex design (see fig. 3). Here, the light is read out by four light sensors. First the light is collected along the plastic edge with the use of a Wave Length Shifter (WLS) fiber (type BCF92). The WLS collects light from shorter sides of the scintillator and propagates it to the light sensors mounted on both sides of the fiber. In both cases, the Multi Pixel Photon Counter (MPPC) devices from Hamamatsu [15] have been used as the light sensors.

Figure 3 shows a conceptual design of a single veto module. It is worth mentioning that each MPPC is mounted directly on a preamplifier PCB to minimize the noise level. The front-end electronics is completed by analog adders, each providing analog sum of signals coming from all sensors of a single paddle. Thus, each paddle provides finally a single electric pulse. Analog adders provide an inverted signal as well.

The frame of KATANA detector is mounted on two trolleys, capable to move on special rails used primarily to set-up the position of the $S\pi$ RIT TPC inside the SAMURAI

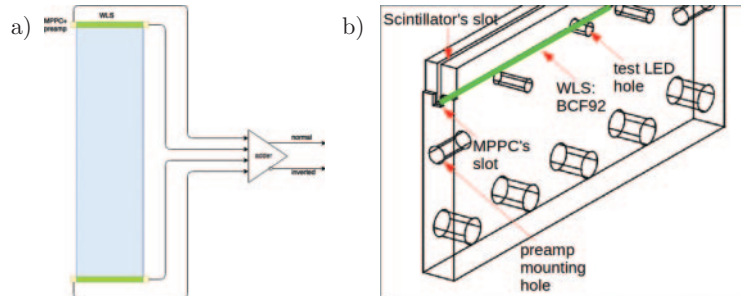


Fig. 3. – a) KATANA single veto module; b) Veto scintillator handle.

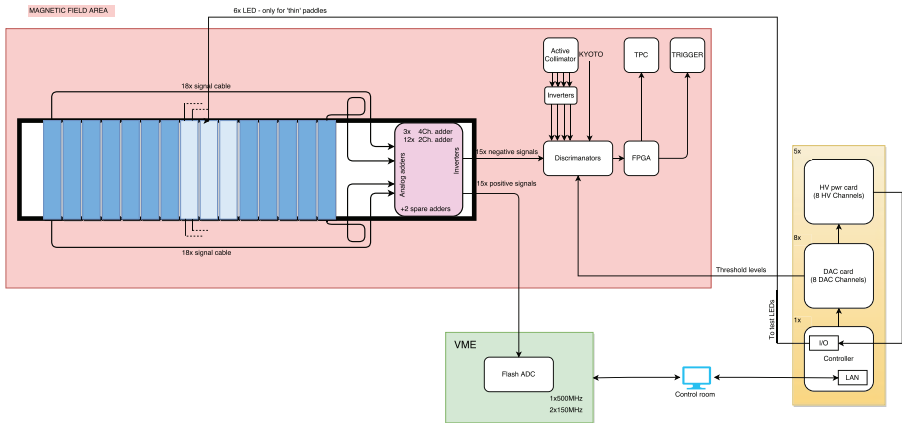


Fig. 4. – KATANA signal wiring.

vacuum chamber. Trolleys provide also possibility for left-right adjustment of the frame (see fig. 2).

4. – Signal path description

Figure 4 shows the distribution of the signal wires. The amplified MPPC's signals of each plastic scintillator are summed, providing one analog signal per each scintillator. Each analog adder has normal and inverted output. In total KATANA provides 15 normal (positive) signals and 15 inverted (negative) ones.

The positive signals are sent to a Flash ADC board (CAEN V1730) for control purpose. The negative signals are dispatched to the leading edge discriminators and are compared to the threshold levels set by remotely controlled DAC cards. The logic outputs of discriminators are then analyzed by a logic circuit built on a FPGA board. The FPGA circuit takes into account discriminated signals from all KATANA paddles (trigger and veto) and additionally, the signals from the Active Collimator and the majority logic signal from the KYOTO array. Its fast and flexible logic allows to provide quickly (within <100 ns) the signals required by the TPC gating grid and by the acquisition system.

5. – Electronics description

5.1. MPPC sensors. – The light readout has been done using the MPPCs of two types. For the thick paddles the S12572-025 product was used. Its photo-sensitive area of size 3×3 mm² consists of 14400 pixels-separate avalanche diodes. The thin paddles are read out by the S12571-010 element, containing 10000 pixels on 1×1 mm² area. Main parameters of the applied MPPCs are specified in table I.

5.2. Preamplifier for MPPC. – A schematic of the preamplifier applied is shown in fig. 5. It consists of a few basic blocks: a common base and a common collector (emitter follower) amplifiers based on the T1 and T2 transistors, respectively; and a simple pole zero cancellation circuit based on the C3, R7 and R8 elements.

TABLE I. – *Main parameters of the applied MPPCs.*

	S12571-010	S12572-025
Photosensitive area	1 × 1 mm	3 × 3 mm
Number of pixels	10000	14400
Typical operating voltage	69 V	68 V
Gain	1.35×10^5	5.15×10^5
Peak sensitivity WL	470 nm	450 nm
Gain temp. coefficient	$1.6 \times 10^3 / \text{K}$	$8.2 \times 10^3 / \text{K}$
Photon detection efficiency	10%	35%

The low-voltage power supplies and filters are omitted in the schematic but it is obvious that high stability and low-noise power supply is required.

The MPPC (D1) is polarized by sufficiently high voltage (HV) provided by high-voltage power supply described below. High frequency signal pulses are passing through C1 to low impedance input of the common base amplifier. This kind of an amplifier was chosen because of its good characteristics for high frequency operation.

A common collector amplifier was used to match the output impedance. The R6 and R9 resistors also play a significant role in this respect. The C2 capacitor cuts off the DC component.

The preamplifier allowed to achieve a one-photon resolution in amplitude. Figure 6 shows the amplitude distribution obtained from a thick paddle, stored in a dark room. The peaks correspond to one, two and more photon, events. It clearly shows sensitivity and amplitude resolution of the thick (trigger) paddles. Of course, during the experiment, the thresholds were set-up much above this natural noise, to detect only light charged particles. On the other hand, the sensitivity of thin (veto) paddles is much lower, as it should give response only for heavy charged fragments.

5.3. HV supply. – The MPPC elements need to be biased. This goal was achieved by designing a dedicated HV power supply, satisfying the following special requirements: 10 mV precision, low noise and low voltage ripple (< 1 mV), 60–80 V range of regulation, 40 channels, remote control via Ethernet, multi-point temperature control, current limiter and a feedback info (saturation/error).

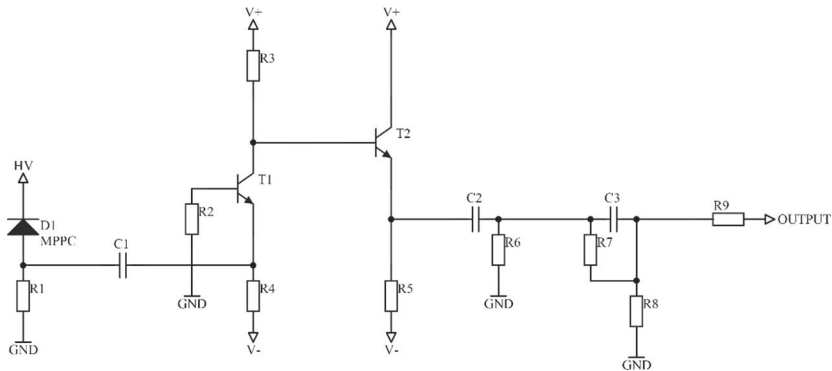


Fig. 5. – Schematic of the preamplifier for MPPC.

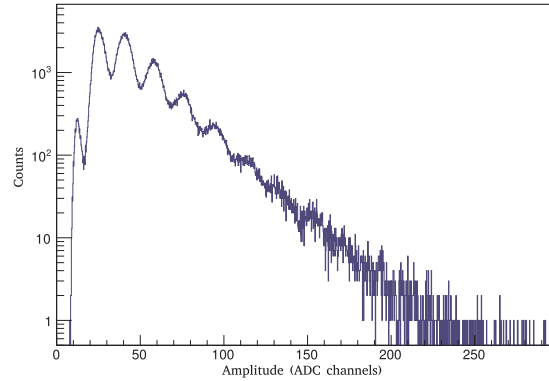


Fig. 6. – Single-photon amplitude resolution achieved for thick paddles, equipped with S12572-025 elements.

Figure 7 presents an actual view of the high voltage power supply (note its modular, expandable construction).

The HV supplier was remotely controlled. The controller was based on a STM32F103 microcontroller with ARM Cortex-M3 core. The Ethernet controller allowed to create a system working in a server mode. The IP and port numbers for the communication are configurable. The interface for the DAC cards and HV cards was custom designed and allowed to connect those cards in parallel. Each card is provided with switches for setting the card address.

The HV supply is temperature sensitive. A DS18B20 element has been chosen as a built-in temperature sensor. This is a digital thermometer with 12-bit ($0.0625\text{ }^{\circ}\text{C}$) resolution and 1-Wire interface for communication. Two such devices were installed inside the high voltage power supply box. Additionally, six such sensors were mounted on the frame of the KATANA detector to monitor the operating temperature of the MPPCs. The temperature data were collected by the controller and were available upon request from the server.

The HV modules on the *HV pwr card* (see fig. 7) can be turned on/off separately

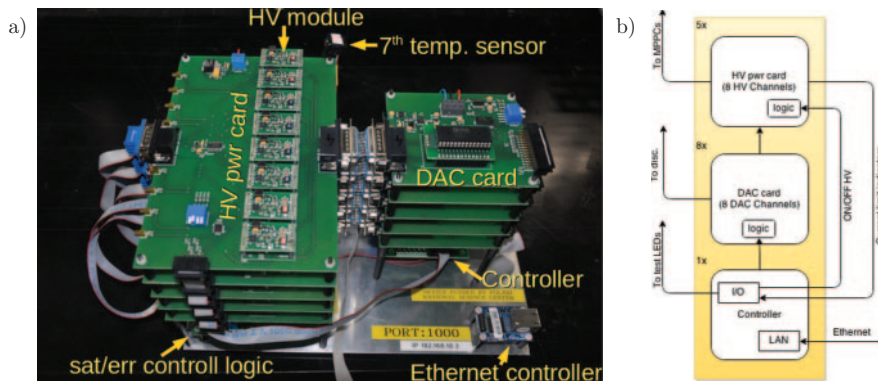


Fig. 7. – HV power supply for the MPPC: a) picture of the device; b) block diagram.

through the controller. Before switching on, the controller sends a code to the specified DAC corresponding to the required voltage. The voltage on the DAC output is a reference voltage for the HV module: the required high voltage appears on the HV module output.

The HV module is based on a MAX1932 APD bias supply and has a flexible design: it can work in analog mode (as described above) or in a “stand alone” mode. In the latter mode a built-in DAC is in use. Nevertheless, our construction is based on external DACs to achieve better parameters. Additional filters were applied as well.

The device is fully controlled through Ethernet and all information about its state can be read out.

Summary

In summary, we have presented technical details of the KATANA detector. The detector was built, tested and used in the recent experiment at RIKEN, playing a significant role in the detection system. Its construction allowed to place it inside strong magnetic field just behind the S π RIT TPC exit window. Fast response, high triggering efficiency, insensitivity to magnetic field, stability and the possibility of remote control were the main attributes of this trigger and veto array.

* * *

Work supported by Polish National Science Center (NCN), Contract Nos. UMO-2013/10/M/ST2/00624 and UMO-2013/09/B/ST2/04064.

REFERENCES

- [1] TSANG M. B. *et al.*, *Phys. Rev. C*, **86** (2012) 015803.
- [2] LI B.-A. and HAN X., *Phys. Lett. B*, **727** (2013) 276.
- [3] RUSSOTTO P. *et al.*, *Phys. Lett. B*, **697** (2011) 471; *Phys. Rev. C*, **94** (2016) 034608.
- [4] LI B.-A., *Phys. Rev. Lett.*, **88** (2002) 192701.
- [5] RIZZO J. *et al.*, *Phys. Rev. C*, **72** (2005) 064609.
- [6] HONG J. and DANIELEWICZ P., *Phys. Rev. C*, **90** (2014) 024605.
- [7] SHANE R. *et al.*, *Nucl. Instrum. Methods A*, **784** (2015) 513.
- [8] JHANG G. *et al.*, *J. Korean Phys. Soc.*, **69** (2016) 144.
- [9] LASKO P. *et al.*, in preparation, arXiv:1610.06682.
- [10] LASKO P. *et al.*, *Proceedings of the 2016 Zakopane Conference on Nuclear Physics*, to be published in *Acta Phys. Pol. B*.
- [11] groups.nscf.msu.edu/hira/NP1306_SAMURAI15/index.htm.
- [12] KOBAYASHI T. *et al.*, *Nucl. Instrum. Methods B*, **317** (2013) 294.
- [13] YANO Y. *et al.*, *Nucl. Instrum. Methods B*, **261** (2007) 1009.
- [14] www.gsi.de/en/work/project_management_fair/rare_isotope_beams/r3b/neuland.htm.
- [15] www.hamamatsu.com.